Communications in Nonlinear Science and Numerical Simulation 119 (2023) 107089

Contents lists available at ScienceDirect

Communications in Nonlinear Science and Numerical Simulation

journal homepage: www.elsevier.com/locate/cnsns

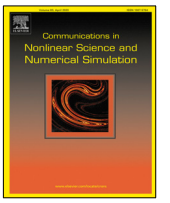

Research paper

Persistence in spatial multi-species food webs: The conflicting influences of isolated food web feasibility and spatial asynchrony

Sean M. Hayes [a,b], Kurt E. Anderson [a,*]

[a] Department of Evolution, Ecology, and Organismal Biology, University of California, Riverside, CA, 92521, USA
[b] Merck and Co. Inc., 126 E Lincoln Ave., Rahway, NJ, 07065, USA

ARTICLE INFO

Article history:
Received 2 August 2021
Received in revised form 14 November 2022
Accepted 1 December 2022
Available online 6 January 2023

Keywords:
Food-webs
Spatial networks
Non-equilibrium dynamics
Persistence
Feasibility
Trophic structure
Body size

ABSTRACT

A central goal of ecology is identifying the mechanisms that allow large, complex food webs to persist. Spatial mechanisms resulting from dispersal connections among local food webs are one factor shown to play a significant role in enabling species persistence, particularly by driving asynchrony in the dynamics among local food webs. However, it is still unknown how these spatial persistence mechanisms operate across food webs. Using simulations of full non-linear food web models, we investigate how spatial persistence mechanisms emerge in multi-species food webs that possess different structural metrics. Specifically, we ask whether 1) spatial persistence mechanisms work similarly across food webs, and 2) if differences can be explained by food web features influencing stability in the absence of dispersal, particularly trophic structure. Food web structures are generated using the allometric niche model that is capable of reproducing realistic feeding patterns and interaction strengths. Our analyses quantify the tendency of modeled food webs to achieve asynchrony in the presence of dispersal and show that this positively affects the ability of species in the food web to persist. We observe an inverse relationship between the ability of food webs to persist when isolated and their tendency to be asynchronous when spatial, indicating a limited ability of food webs that persist when isolated to benefit from spatial persistence mechanisms. Our results demonstrate a relatively unexplored layer of food web properties which determine the ability of a food web to capitalize on the stabilizing opportunities created by dispersal, specifically those that influence the tendency for dispersal-linked food webs to be asynchronous. Future studies should expand on our results by examining how properties of spatial connections and food webs influence the ability of food webs to achieve asynchrony.

1. Introduction

Identifying the mechanisms that allow large, complex food webs to persist has been a central goal of ecology since the work of Robert May (1972) first demonstrated that high species diversity and interaction complexity reduces stability on species persistence in model ecological communities. Since May's early pioneering work, extensive research has been conducted on which structural components of food webs impart stability required for species persistence in food webs [1]. Many food web properties have been shown to play a major role in species persistence, such as having a

* Corresponding author.
E-mail address: kurt.anderson@ucr.edu (K.E. Anderson).

https://doi.org/10.1016/j.cnsns.2023.107089

few strong interactions balanced by many weak ones [2,3] and having high ratios of body sizes between consumers and resources [4,5]. These mechanisms operate by leading to an overall reduction in the average interaction strength between species that in turn increases food web stability. Large and empirically realistic differences in body sizes have a particularly strong effect of weakening the strength of consumer–resource interactions, enhancing species persistence in food webs [6,5,7].

The majority of early studies of food web persistence, including those mentioned above, focused on isolated food webs in the absence of spatial connectivity. However, spatial connectivity and dispersal among local communities has been increasingly shown to play a significant role in enabling species persistence [8–10]. The spatial persistence mechanisms enabled by dispersal among food webs range from dispersal increasing low densities of extinction-prone species [11,12], to reducing population variability through averaging effects [13], to reducing the effect of disturbances [14,15] and averaging environmental heterogeneity [16,10]. For dispersal to have any effect however, it is typically also necessary that the connected food webs differ in structure or dynamics. For a species to be rescued from extinction in a location, the times at which its populations in dispersal-connected locations are vulnerable must be staggered, requiring differences in the timing of fluctuations in abundances. Dispersal from locations with lower variability and extinction risk can also moderate the fluctuations of highly variable or extinction prone ones. These differences in timing and dynamics, or 'asynchrony', are thus a critical component of the spatial persistence mechanisms relied upon by many complex food webs [17–19].

Studies of spatial food webs suggest that spatial interactions influence species in ways that may not be readily predictable from analysis of food webs in isolation [20,16,10]. Spatial asynchrony in food web dynamics necessary for many spatial persistence mechanisms may emerge from unstable species interaction models, where large-amplitude cycles may be driven out of phase across sites by low levels of dispersal [21,22,12], although Turing-like instabilities may arise in spatial models that are stable in the absence of dispersal [23,24]. Thus, non-spatial and spatial mechanisms may not promote food web stability in the same contexts. In particular, it is unknown whether mechanisms that support species persistence when spatially isolated, for example high consumer–resource body-size ratios, operate when food webs are connected to one another by dispersal.

Thus far spatial persistence mechanisms have primarily been studied for small food web modules [25–27] due to the many inherent challenges both in formulating realistic models with large numbers of interacting species and in characterizing the dynamics of large food webs. These studies have tended to aggregate food webs by the number of species or patches in their analyses or by examining dynamics near equilibrium [16,10,24]. Models based on colonization/extinction dynamics have shown that food web modules exhibit different responses to habitat loss [25,28]. However, such models omit biomass dynamics such as population cycles which may play an important role is spatial consumer/resource interactions [22]. Thus, despite the insights provided by previous work, it is still unclear how the action of spatial persistence mechanisms differs between specific food webs based on the structure of trophic interactions.

We investigated how spatial persistence mechanisms operate across a range of food webs with different structural features known to influence food web stability in the absence of dispersal, namely species number, number of trophic levels, and consumer–resource body-size ratios. We asked whether (1) spatial persistence mechanisms work similarly across food webs, and (2) if differences can be explained by food web features influencing stability in the absence of dispersal, particularly trophic structure. Ecologically-realistic food webs were generated with an allometric modeling framework [29,4] that utilizes body size and metabolic type to constrain parameter values and species interaction strengths to realistic values. Underlying food web interaction structures were generated by the niche model that is able to reproduce realistic patterns in natural food webs [30]. Our analyses quantified the tendency of various food webs to achieve asynchrony in the presence of dispersal and the resulting effects on the ability of species to persist. We observe an inverse relationship between the ability of food webs to persist when isolated and their tendency to be asynchronous when connected by dispersal, limiting the ability of food webs that are persistent when isolated to benefit from spatial persistence mechanisms. As a result, the overall persistence of spatial food webs is determined by a complex interplay between the trophic structures that enhance the ability of a given food web to persist when isolated and the action of spatial coexistence mechanisms.

2. Methods

2.1. Model formulation

We modeled the dynamics of spatially explicit food webs using an allometric consumer–resource model [29,4] extended to include dispersal and generalized for i species and p patches (Table 1):

$$\frac{dB_{i,p}}{dt} = F(B_{i,p}) + G(B_{i,p}) - H(B_{i,p}) - I(B_{i,p}) + J(B_{i,p})$$

$$F(B_{i,p}) = B_{i,p} a_{r,i} M_i^{-.25} \left(1 - \frac{B_{i,p}}{K_{i,p}}\right)$$

$$G(B_{i,p}) = B_{i,p} a_{x,i} y_i M_i^{-.25} \frac{\sum_{j=1} \omega_{i,j} B_{j,p}^h}{B_0^h + \sum_{j=1} \omega_{i,j} B_{j,p}^h}$$

Table 1
Definitions of model components for the spatially explicit food web model in Eq. (1) and ranges used in model simulations.

Model component	Description	Range or Value
State variables		
$B_{i,p}$	Biomass of species i in patch p	
Functions		
$F(B_{i,p})$	Resource biomass production rate	
$G(B_{i,p})$	Consumer biomass production rate	
$H(B_{i,p})$	Biomass lost to consumption	
$I(B_{i,p})$	Biomass lost to metabolic processes	
$J(B_{i,p})$	Net biomass change from dispersal	
Parameters		
M_i	Body mass for species i	$M_R 10^{ZT_i}$
M_R	Basal resource body mass	[0.1]
Z	log_{10} consumer–resource body size ratio	[2]
T_i	Trophic level of species i	[0,4]
$a_{r,i}$	Resource mass-specific biomass growth rate	[1]
K_i	Resource carrying capacity	[1]
$\omega_{i,j}$	Relative effort species i spends consuming species j	[0,1]
$a_{x,i}$	Consumer mass-specific metabolic rate	[0.88]
y_i	Metabolic scaled maximum consumption rate	[4.0]
$e_{i,j}$	assimilation rate for species i feeding on species j	[0.65]
B_0	Consumer functional response saturation constant	[0.5]
h	Consumer functional response shape parameter	[1.0]
d_i	Dispersal rate among patches	[0.001]

$$\begin{aligned} H(B_{i,p}) &= \sum_{j=1} \frac{B_{j,p} a_{x,j} y_j M_j^{-.25} \omega_{j,i} B_{i,p}^h}{e_{j,i}[B_0^h + \sum_{k=1} \omega_{j,k} B_{k,i}^h]} \\ I(B_{i,p}) &= B_{i,p} a_{x,i} M_i^{-.25} \\ J(B_{i,p}) &= d_i \sum_{q=1} L_{q,p} B_{q,p} \end{aligned} \tag{1}$$

where $B_{i,p}$ is the biomass of species i in patch p. In the formulation above, a given species i can represent a resource or consumer. The function F defines the rate of production in the resource, G is a consumer's consumption-dependent biomass growth rate, H the biomass lost by either resources or intermediate consumers from consumption, I the biomass lost owing to metabolic processes, and J is the net change in a population due to immigration and emigration. For resources G and I are set to 0, and likewise F is set to 0 for consumers.

Production rates in the allometric model were scaled by body mass; M_i is the average body mass for species i. For resource species i, $a_{r,i}$ is the mass-specific biomass growth rate and K_i the carrying capacity. For consumer species i consuming species j, $a_{x,i}$ is its mass-specific metabolic rate, $\omega_{i,j}$ is the relative effort species i spends consuming species j, y_i is its maximum consumption rate relative to its metabolic rate, and $e_{i,j}$ its assimilation rate. The type II functional response of consumers is additionally defined by the half-saturation coefficient B_0 and the shape parameter h.

We used a single set of physiological parameters across patches p and simulations to limit model complexity. The resource parameters $a_{r,i}$ and K_i relate only to the time scale of dynamics and baseline resource enrichment level respectively. As there is a single basal resource, we set both $a_{r,i}$ and K_i to 1 for all patches without loss of generality. Patch-level resource carrying capacity K_i was held constant across isolated and dispersal connected patches rather than re-scaling it to match a change in patch number in order to focus on the effects of dispersal connectivity [20,16,10].

For consumers, $a_{x,i}$ = 0.88, y_i = 4.0, and $e_{i,j}$ = 0.65, which corresponds to a case where the food web is composed of invertebrates and omnivorous vertebrate ectotherms that has been well-studied previously [4,31]. We also used B_0 = 0.5 and h = 1.0 for the consumer functional response. These parameter choices generate limit cycles that are highly sensitive to the effects of dispersal to emphasize the effects of spatial connectivity on food web dynamics.

Interactions between species were defined by the matrix ω with elements $\omega_{i,j}$; each column j sums to 1, which is the total effort each consumer species has to allocate. The interaction matrix ω was generated using the niche model [30] due to both its success in reproducing many of the properties of real food webs and its ease of computation. Skewed interaction strengths are known to strongly affect stability in model food webs [2,32]; we therefore used the simplifying assumption that the relative feeding effort was split evenly between all of a consumer's available prey to standardize this effect across food webs examined.

We simulated dynamics for food webs consisting of four to six species, attempting to use all possible food web configurations for these numbers of species by exhaustively sampling the niche model until no additional unique food webs could be readily found. Food webs which included symmetric feeding links (two species feeding on one another)

Fig. 1. Dispersal structure used for all spatial simulations. Each circle represents a patch p which contains an identically structured local food web, with each gray line to a neighboring patch q specifying an unbiased dispersal connection. This structure can be thought of as two symmetrical modules of five local food webs each, with three interior food webs connected to every other patch in the module and two exterior food webs which connect to their opposite exterior patch.

were omitted. Following the methods of [4], all food webs were also constrained to one resource, keeping the total potential energy supply constant among all food webs. This allowed us to focus on the effects of the interaction structure rather than differences in the resource base among food webs.

From the interaction matrix ω we defined each species' trophic level T as the shortest path distance from the basal resource. This value was then used to define the body mass M_i for species i as $M_i = M_R 10^{ZT_i}$ [4], where $M_R = 0.1$ is the mass of the basal resource and Z is the $\log_{10}$ consumer–resource body mass ratio. We used $Z = 2$, an intermediate value which allows for oscillatory dynamics and many food webs reliant upon spatial persistence mechanisms while still allowing a robust potential for species to coexist.

Local food webs were connected to one another via dispersal. Food webs were only connected to food webs with similar structure within individual simulations (i.e., there was no a priori spatial heterogeneity in food web structure). Dispersal connections between populations were encoded by the Laplacian matrix **L**, where each element $L_{p,q}$ denotes the presence of a dispersal connection between patches p and q with 1 or is otherwise 0. For connected patches $L_{p,q} = 1$, the amount of dispersal was given by each species' dispersal rate d_i. The diagonal elements $L_{p,q}$ are the negative sum of dispersal from patch p ($-L_{p,p} = L_{.,p}$), representing emigration.

For our simulations we used a single spatial structure (Fig. 1) to remove any confounding effects of variation in spatial structure, focusing only on the effect of variation in food web structure. The spatial structure we used had ten patches, the smallest number we found to be able to readily support asynchrony under the conditions of our simulation. For the specific structure, we chose a regular structure in which each patch is linked by dispersal to the same number of other patches (patch "degree"). Specifically, each species in each patch can immigrate to and emigrate from four other patches, and dispersal connections are always symmetric such that $L_{p,q} = L_{q,p}$. While many other spatial structures could potentially be used, regular structures add the constraint that all communities are functionally identical. Additionally, the structure we selected was shown in previous work to have a high tendency towards asynchrony among the set of all ten-patch regular spatial structures [33].

Each species i disperses among patches encoded in the Laplacian matrix L with dispersal rate d_i. We set dispersal $d_i = 0.001$ for all species and simulations, an intermediate value for which asynchrony is common but not guaranteed [33].

2.2. Simulation methods

We generated dynamics for each food web under random initial conditions, with each population's starting density chosen uniformly from the interval [0.2, 1.8]. This range was chosen as a relatively variable set of initial conditions that could produce asynchrony when asynchrony was possible, but within the typical ranges of abundances observed for most species in our simulations. Simulations lasted for 60000 time steps, as food webs were found to reach steady state dynamics by $t = 50000$. The remaining 10000 time steps were then used to assess steady state dynamics. This procedure was then replicated 100 times for each spatial food web. The dynamics of each food web were also simulated in the absence of dispersal 1000 times (the number of spatial simulations times the number of local food webs in spatial simulations) to provide an effective comparison for the effects of space on the dynamics of each food web. Simulations were carried out in C++ using the FORTRAN Odepack solver lsoda [34,35].

2.3. Characterizing persistence and asynchrony

Each simulation was characterized in terms of feasibility, minimum population sizes, and asynchrony among patches. Both feasibility and minimum population size are two population dynamic measures that describe whether a food web is capable of supporting the persistence of all species and, among feasible food webs, the extinction risk of each species during steady state if environmental or demographic stochasticity were present, as they would be in nature. Asynchrony in contrast is that is hypothesized to support spatial food web persistence when dispersal connected.

First, we determined whether food webs in each simulation were *feasible*, where a feasible food web was one in which all species achieved a positive steady state (i.e., there were no extinctions). The steady state in all of our simulations was an oscillatory one; therefore, each species' abundance had to be positive at all points in the population cycle. As

abundances were modeled as continuous state variables, they could become arbitrarily small and still remain strictly positive. Therefore, we set a non-zero extinction threshold below which a population was considered extinct. We chose $B_{i,p} = 1 \times 10^{-10}$ as our extinction threshold, meaning that feasibility was obtained when at least one population for each species in the food web maintained an abundance higher than 1×10^{-10} at all times.

Second, if a food web reached a feasible steady state as defined above, the minimum regional abundance of each species during steady state was calculated. These minimum regional abundances (species minima) were calculated over the final 10000 time steps of each simulation. Minima were calculated as regional values such that abundances were summed across all patches for each species. Species minima were then scaled by the number of patches (ten if spatial, one if non-spatial), effectively re-scaling abundances such that the patch size of the non-spatial control was comparable to the combined size of all patches for the spatial food webs. Food webs as a whole were characterized in terms of the species with the lowest total regional species minima.

Finally, we characterized asynchrony by comparing abundances among patches and the number of synchronized clusters that they produced once simulations had reached steady state. Two food webs were considered synchronized if the abundances for each species in the first patch were within 0.01 of the corresponding species in the other patch at each time step during the assessment period. While this is a strict definition of synchrony, it was found to produce the same results as comparable procedures for determining synchrony in deterministic simulations [22] while being simple to compute. To minimize computation length, asynchrony was calculated using the last 20 time steps of each simulation. This time series length was able to provide consistent results with those calculated using longer time series. Sets of synchronized food webs were grouped together in clusters, where each synchronized cluster was a set of synchronized food webs with dynamics that were unique from other clusters. An asynchronous steady state with ten clusters would have all food webs exhibiting unique dynamics and therefore no synchrony, while a steady state with one single cluster would reflect complete synchrony across all food webs.

To explain differences in isolated feasibility among six-species webs, we considered consumer–resource body size ratios which have been shown to play an important role in the stability of allometric food web models [4]. Recall that the consumer–resource body size ratio R_{ij} for each feeding link ($\omega_{ij} > 0$), where j feeds on i, is given by

$$R_{ij} = M_j/M_i \tag{2}$$

where M_j and M_i are the body masses of species j and i respectively.

The assigned average value in our food webs is $Z = 2$, yet the individual values for each consumer–resource pair and the actualized average value will vary across simulated food webs. Thus, the effects of trophic level and body-size ratios on persistence and synchrony may be confounded with the number of trophic levels in our size-structure communities. Therefore, we introduce a metric that adjusts trophic level based on the body size ratio for each feeding relationship. Specifically, we characterize species in terms of their participation in feeding relationships that lead to maximum body size ratios ($R = 10^2$) by the following metric:

$$\psi_j = \sum_{i=1} \dot{\omega}_{ij}\psi_i$$

where

$$\dot{\omega}_{ij} = \begin{cases} \omega_{ij}, & \text{for } M_j > M_i \\ 0, & \text{for } M_j \leq M_i \end{cases} \tag{3}$$

Additionally, ψ is set to 1 for basal resources. The calculation of this metric removes all links where consumers are smaller or equal in size to their resources, and includes each resource's participation in optimal feeding relationships as well. By including the feeding relationships of each consumer's resource, this metric emphasizes chains of maximum body size ratio feeding relationships, with the maximum value ($\psi_j = 1$) reached only if every interaction in each chain leading back from species j to the basal resource has $R_{ij} > 1$. This metric allows us to define a consumer–resource body size ratio adjusted trophic level $T_{i,adj}$ for each species j as

$$T_{j,adj} = (T_j - 1) + \psi_j. \tag{4}$$

Fig. 3 illustrates the use of this metric using the example of six species food webs with four trophic levels. Higher values of $T_{i,adj}$ have stronger chains of interactions among species with high consumer–resource body size ratios which are known to be stabilizing in food web models [4].

3. Results

We identified 18 food webs that were capable of supporting the coexistence of all original species (Fig. 2); these food webs were used for further analyses. These food webs were feasible much more often in dispersal connected treatments than in isolation, with eleven out of the eighteen food webs only able to persist in the presence of dispersal.

The persistence effects and patterns of asynchrony observed in the presence of dispersal differed among food webs examined. Persistence via asynchrony was most common in the food webs which were not feasible when isolated (e.g. food webs d–g, i–k, m, and o; Fig. 4). Two four-species webs (a and b) did show relatively high feasibility in isolation

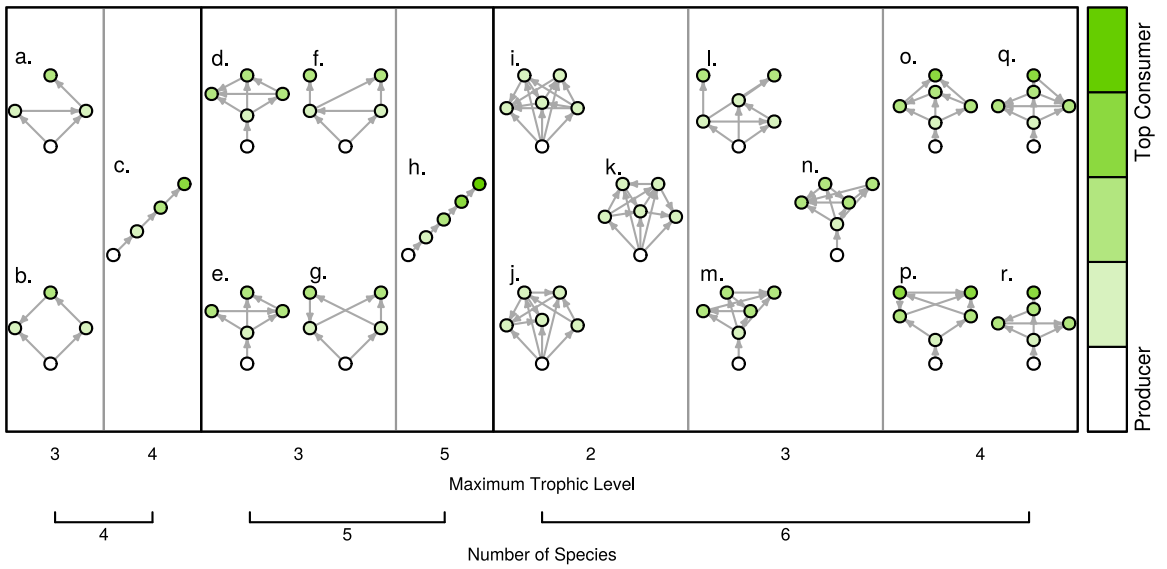

Fig. 2. Illustration of all food webs which were feasible in at least one simulation that were included in further analyses. The direction of arrows indicates the flow of energy, such that $B_1 \rightarrow B_2$ indicates that B_1 is eaten by B_2. Darker circles are species that are higher in the food web, meaning that there are more feeding links between them and the basal resource.

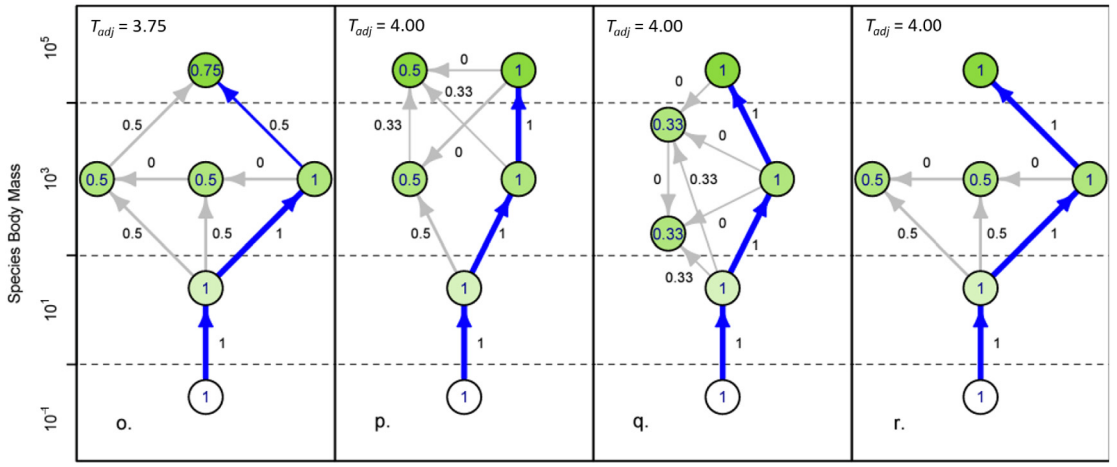

Fig. 3. Illustration of body size, trophic level, and interaction strengths in six species food web structures. Each node represents a species i labeled with its metric for participation in feeding relationships with larger consumers and smaller resources, ψ. Each arrow represents a feeding interaction such that $i \rightarrow j$ indicates j eats i, labeled with size ratio adjusted interaction strength $\dot{\omega}_{ji}$. The adjusted interaction strength $\dot{\omega}_{ji}$ is 0 if the body size of the resource is equal or greater than the body size of the consumer, and equal to the original interaction strength ω_{ji} otherwise. The interactions highlighted in blue indicate the strongest food chain between a species of the top trophic level and the basal resource. The body size adjusted trophic level $T_{i,adj}$ based on this food chain is also given for each food web. Food webs p., q., and r. have the same maximum unadjusted trophic level and each have a strong food chain of made up of interactions with body size ratios R greater than one. By contrast, food web o.'s top species connects a chain with high R values and chains with low R values, leading to a lower $T_{i,adj}$ value.

and very high feasibility when dispersal connected, whereas most of the food webs we examined which were feasible when isolated had relatively low frequencies of feasibility either when isolated or when dispersal connected (e.g. food webs h, p, and q; Fig. 4) compared to food webs which were only feasible with dispersal.

Higher asynchrony, quantified by the number of distinct clusters, was most frequent in the food webs which were not feasible when isolated. Most food webs were able to produce multiple distinct patterns of spatial clustering, where each synchronized cluster represented a set of synchronized food webs with unique dynamics (Fig. 4). Food webs which tended to be at least feasible in isolation, particularly c., p., q., and r., also did not typically show asynchrony in the presence of dispersal.

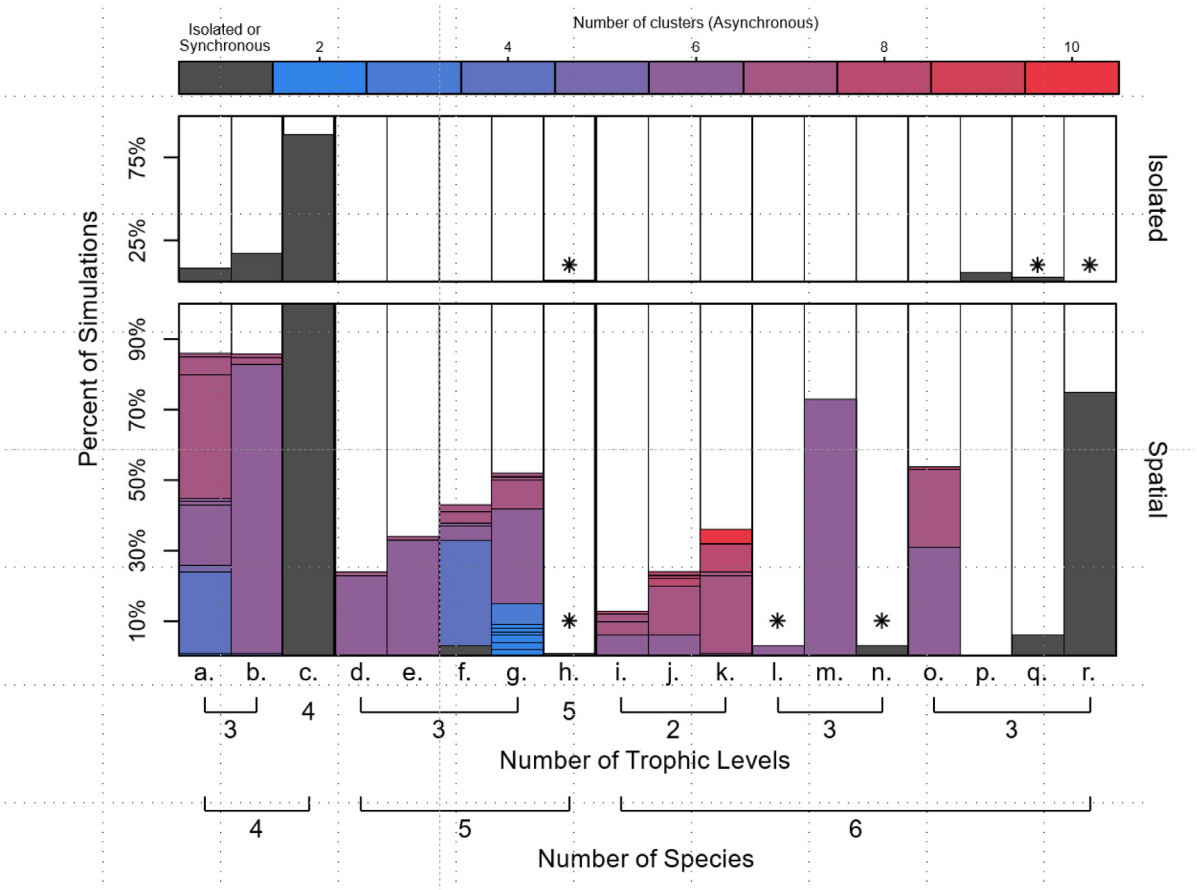

Fig. 4. Comparison of the percentage of simulations with feasible food webs when isolated and when connected spatially by dispersal. Each spatially connected set of food webs were simulated 100 times while each food web was also simulated without dispersal 1000 times. A (*) symbol denotes that a food web is feasible for a given treatment but only rarely, specifically in less than 5% of simulations. Food webs are feasible much more often when spatially connected, with many only reaching feasible equilibrium with these connections. Each synchronized cluster is a set of synchronized food webs with unique dynamics, thus the number of clusters is the number of unique sets of dynamics present among patches for a given equilibrium. When spatially connected, many food webs produce stable asynchronous dynamics with multiple patterns of clustering. However, food webs which are feasible when isolated rarely exhibit asynchronous dynamics.

Simple metrics of trophic structure showed limited ability to explain differences in persistence and spatial dynamics among food webs. The highest maximum trophic level and average consumer–resource body size ratios are found in linear chain food webs (Table 1). While the four species food web c. is the only food web which is synchronous in the presence of dispersal, the percentage of feasible runs in the five species linear chain food web h. was small and six-species linear food chains were never feasible and so could not be included in our analyses. The three six-species webs that were feasible in isolation and synchronous when dispersal connected (p., q., r.) had the highest maximum trophic level observed among feasible six-species webs (four). Yet, one other six-species food web (o.) was not feasible in isolation and exhibited high asynchrony when dispersal connected. This food web has the same number of trophic levels as those previously mentioned and a *higher* average body size ratio.

While individually both the number of trophic levels and the average consumer–resource body size ratio fail to explain the difference in feasibility and synchrony among food webs, a clear difference can be found when adjusting trophic level based on the body size ratio for each feeding relationship (Table 2). All food webs with $T_{adj} \geq 4$ are feasible in at least some simulations when isolated and synchronous when dispersal connected. Thus, chains of feeding relationships between larger consumers and smaller resources is associated with food web feasibility when isolated, consistent with previous allometric food web models [4]. From this comparison we can see that food webs p., q., and r., which are feasible when isolated and synchronous when spatial, each have a species in the fourth trophic level where $\psi_i = 1$. Thus, these food webs contain a chain of maximum stabilizing feeding relationships back to the basal resource. By contrast, the top species in food web o. has $\psi = 0.75$; this food web is not feasible when isolated and asynchronous when dispersal connected.

The benefits of high T_{adj} for food web feasibility, however, are complex. When T_{adj} is low, increases in this metric corresponded to increases in food web feasibility, particularly among food webs that exhibit asynchrony in their

Table 2
Metrics of food web structure for food webs in Fig. 2. The average consumer–resource body size ratio R and maximum trophic level alone do not predict feasibility of isolated food webs. In contrast, isolated food webs with long chains of high consumer–resource ratios that lead to a body size adjusted trophic level $T_{i,adj} \geq 4$ are feasible in at least some simulations.

	Species #	R	Maximum trophic level	T_{adj}
Feasible when isolated				
c.	4	10^{2}	4	4.00
h.	5	10^{2}	5	5.00
p.	6	$10^{1.75}$	4	4.00
q.	6	$10^{1.88}$	4	4.00
r.	6	$10^{1.86}$	4	4.00
Not feasible when isolated				
a.	4	$10^{1.88}$	3	2.5
b.	4	$10^{1.88}$	3	3.00
d.	5	$10^{1.76}$	3	3.00
e.	5	$10^{1.83}$	3	3.00
f.	5	$10^{1.92}$	3	2.75
g.	5	$10^{1.92}$	3	3.00
i.	6	$10^{1.56}$	2	2.00
j.	6	$10^{1.63}$	2	2.00
k.	6	$10^{1.59}$	2	2.00
l.	6	$10^{1.88}$	3	3.00
m.	6	$10^{1.75}$	3	3.00
n.	6	$10^{1.70}$	3	3.00
o.	6	$10^{1.88}$	4	3.75

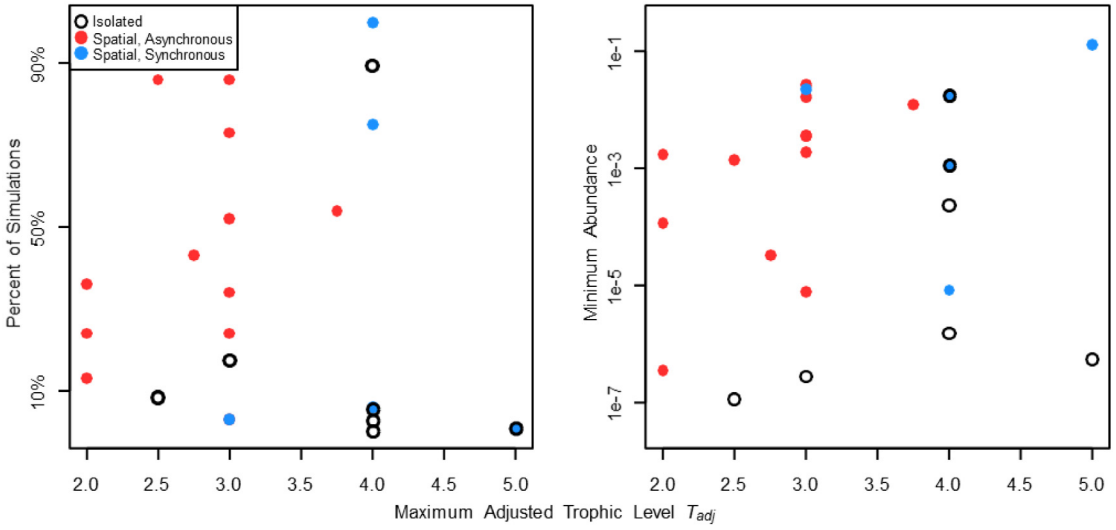

Fig. 5. Comparison of each feasible food web's maximum consumer–resource body size ratio adjusted trophic level T_{adj} with food web persistence metrics. The percent of simulations with feasible food webs (left panel) are as shown in Fig. 3. The minimum abundances presented (right panel) are calculated from the total abundance of each species across all connected patches, and scaled by the total number of patches to enable comparison between isolated and spatial treatments. The most vulnerable species is the species for each food web with the lowest minimum abundance. These minimum abundances are averaged across all isolated, spatially synchronous, or spatially asynchronous steady states observed for each food web.

spatial dynamics (Fig. 5). As T_{adj} continues increasing however, food web dynamics shift from largely asynchronous to synchronous. Once this shift occurs, food webs now exhibit at least some feasibility when isolated but the overall proportion of feasibility across simulations drops. The increase in feasibility across all foods webs is supported by increases in the minimum abundances of constituent species (Fig. 5), as there is a weak but consistent positive relationship between

T_{adj} and the minimum average abundance of any species in each food web. This pattern holds across shifts in food web dynamics from feasibility through spatial asynchrony to feasibility in isolated and spatially synchronous food webs.

To complicate matters further, it appears in some cases that spatial dynamics can enable dispersal connected food webs to reach a synchronous equilibria with dynamics that are not simply a sum of dynamics exhibited in isolation. Specifically, the minimum abundance in the five species linear food web h. shifts from $10^{-6.26}$ when isolated to $10^{-0.88}$ in the presence of dispersal, despite synchronous spatial dynamics. This could be due to a given food web having multiple alternative isolated equilibria with one that is favored due to an effect of dispersal on the transient dynamics. While this effect could play a role in changing the feasibility in some food webs, others receive no benefit, creating yet another dimension of variation in the response of differing food web structures to dispersal that is unaccounted for in the trophic metrics we examine.

4. Discussion

Taken together our results illustrate clear variation in asynchrony among food webs, with asynchrony being uncommon in food webs which are feasible in isolation. As a result, substantial differences in the benefit each food web experiences from spatial coexistence mechanisms emerge. This relationship between the prevalence of asynchrony and structure is best predicted by the maximum consumer–resource body size ratio adjusted trophic level T_{adj} for each food web, where species with long chains of high consumer–resource body size ratios showing the greatest isolated food web feasibility. However, the ultimate effects of dispersal and spatial persistence dynamics are not as well predicted by any metric. The ability of food webs to persist when connected by dispersal changes dramatically compared to persistence when isolated, due to the emergence of negative feedbacks between the mechanisms which promote persistence in isolation versus in spatial environments and the ability of food webs to switch to alternative equilibria, both synchronous and asynchronous.

Asynchrony in our models differs from what has been commonly discussed in the ecological literature in that it is not the result of a spatially heterogeneous environment [36,37,16] or variation in dispersal ability among species [26,38,39]. Rather, we assume all patches are identical and dispersal is equal for all species. The asynchronous equilibria we observe therefore emerge purely from the interactions between local food webs via dispersal. Such self-organizing patterns have been observed in distributed systems across many fields. In some cases, asynchronous patterns may emerge from dispersal driven destabilization of a homogeneous steady state [40,41], while in others asynchronous oscillatory steady states may coexist with synchronous ones with endpoints determined by initial conditions [42,43]. Different patterned steady states in our food web models are quantified by different numbers of asynchronous clusters observed. Most of our food webs exhibited more than one cluster states that arose due to variation in initial conditions (Fig. 4); multiple cluster states have been observed in simpler food web models on multiple types of dispersal networks [22,33,44,45]. Regardless of generating mechanism, the asynchronous equilibria which result from pattern formation in ecological systems have been shown to reduce fluctuations in population abundances relative to synchronized equilibria [22,27,33], as they do for most of the food webs in our simulations.

While it has been previously demonstrated that asynchrony depends strongly on the structure of dispersal connections within simple food webs [22,27,23], our results show that asynchrony depends on the structure of interactions within food webs as well. Moreover, the strongest determinant of a food web's ability to form stable asynchronous patterns appears to be the inability to persist in isolation. Considered in terms of pattern formation, this is actually the expected result: the most commonly invoked mechanism for the formation of asynchronous patterns is the destabilization of the synchronized, homogeneous state known as the Turing instability [40]. The inverse relationship between extinction risk of local populations and persistence of multiple dispersal linked populations was referred to as the "spatial hydra effect" by [12] and has been explored in simple two-species predator–prey models [46,47].

Our results illustrate similar behavior in more complex, multi-species food webs. In the context of our food web simulations, food webs which can persist in isolation are guaranteed to have a stable synchronized equilibrium, as this equilibrium will effectively produce the dynamics of a single large isolated patch. Thus when a food web with a stable synchronous equilibrium is in a spatial environment, any asynchronous equilibria must compete with the synchronous one. The more stable the synchronous equilibrium is, in terms of the tendency of the system to return to it following a perturbation, the less likely it is to escape it and reach an asynchronous equilibria. This is illustrated in the comparison between food webs a. and b. and food web c. in Fig. 4. Food webs a. and b., which are not often able to return to synchrony following perturbation, switch to asynchronous equilibria when connected by dispersal, while food web c., which is almost always able to return to equilibrium without extinction when isolated, remains synchronous when dispersal connected.

The inverse relationship we observe between a food web's ability to persist when isolated and to become asynchronous via pattern formation makes predicting the ability of food webs to persist in spatial environments challenging. In our simulations we observe that the maximum consumer–resource body size ratio adjusted trophic level ψ, a measure of structure that emphasizes strong chains of interactions between species with high consumer–resource body size ratios, is a good predictor of persistence in isolated food webs. This agrees with previous results investigating the persistence and stability of isolated food webs [4]. The results of our spatial simulations complicate the relationship between body size and persistence however. When dispersal is present, food webs with lower ψ values, indicating a weaker backbone of strong, high body size ratio trophic interactions, often have a comparable if not superior ability to maintain species persistence

relative to those with higher values because of the stronger effects of spatial persistence mechanisms. Other examples of context-dependent effects of food web properties have been noted previously when compared across a gradient of dispersal strength, particularly the number of species [20] and proportion of weak trophic interactions [13]. Our work builds upon these observations by specifically demonstrating that context-dependent effects of food web properties can result due to how these properties influence spatial asynchrony.

Our results suggest that both non-spatial and spatial mechanisms are likely to be important in stabilizing natural food webs, although perhaps having different effects depending on context. The body-size adjusted trophic level T_{adj} is one measure that potentially guides how important dispersal connections might be for a given food web. Lower values of T_{adj} that indicate less dominance by strong chains of consumer–resource interactions with high body size rations may point to a greater need to consider dispersal as a stabilizing factor. Despite increasing interest in spatial mechanisms of stability, most theoretical and empirical research continues to explore food webs in the absence of dispersal. Recent work has particularly focused on including a broader range of ecological interactions into food web models [48–51]. Determining how these additional components of food webs interact with dispersal to influence stability is an ongoing needed area of future research.

We used a single dispersal rate and spatial dispersal network in our simulations and assumed these were shared by all species in the food web. All of these have been shown to have strong effects which could alter the dynamics we observed. Dispersal is a form of coupling among oscillators that tends to promote asynchrony at intermediate levels [21,52,22,45]. Isolated food webs did not benefit from persistence mechanisms made possible by dispersal (Fig. 4), but increasing dispersal would most likely lead to synchronization of dynamics that would also negatively influence persistence [20]. Changes in dispersal network structure also influence persistence [53]; however, dispersal structure may produce complex patterns of asynchrony that are more challenging to predict than changes in coupling strength [22,33,44,54], and determining the effects of dispersal network structure remains a major challenge [55]. Variation in dispersal rates among species is also likely common in food webs and may be related to body size [38,56–58]. Models show that consumer movement [24,59] or greater dispersal among larger bodied species [60,61] can stabilize spatial food web dynamics with local variation in environmental conditions. In contrast, variation in dispersal among species can also be destabilizing in spatially homogeneous systems [24,62–65]. Reconciling these patterns and integrating them with a broader theory of dispersal variation on complex networks remains an ongoing challenge [55].

Altogether our findings strongly suggest that a food web's persistence when isolated cannot readily predict its persistence in the presence of dispersal connections; if anything, these properties are in opposition to one another. There appears to be an additional but relatively unexplored layer of food web properties which determine the ability of a food web to capitalize on the stabilizing opportunities created by dispersal, specifically those that influence the tendency for dispersal-linked food webs to be asynchronous. More investigation is needed to generalize these findings beyond the specific cases we explore however. Further study expanding these results to include the effects of spatially heterogeneous environments and variation in the ability of species to disperse on the ability of food webs to achieve asynchrony in particular is important moving forward. Nevertheless, our results represent an important step forward by shedding light on the role of asynchronous pattern formation in determining the persistence of food webs in space. Given the ubiquity of dispersal in real food webs and the rapid alteration of the spatial environment due to human activity, it is more important than ever to understand the role of spatial dynamics in enabling the persistence of species in nature.

CRediT authorship contribution statement

Sean M. Hayes: Conceptualization, Methodology, Software, Formal Analysis, Data curation, Writing – original draft, Writing – review & editing, Funding acquisition. **Kurt E. Anderson:** Conceptualization, Methodology, Resources, Writing – review & editing, Supervision, Funding acquisition.

Declaration of competing interest

The authors declare that they have no known competing financial interests or personal relationships that could have appeared to influence the work reported in this paper.

Data availability

Code used for models has been placed in a public repository and cited in the manuscript.

Acknowledgments

KEA was supported by National Science Foundation, USA grant DEB-1553718. SMH was supported in part by an award from the Shipley-Skinner Reserve-Riverside County Endowment administered through the UCR Center for Conservation Biology, USA. The authors thank two anonymous reviewers whose comments improved this work.

References

[1] McCann KS. The diversity–stability debate. Nature 2000;405(6783):228–33.
[2] McCann KS, Hastings A, Huxel GR. Weak trophic interactions and the balance of nature. Nature 1998;395(6704):794–8.
[3] Neutel A-M, Heesterbeek JA, De Ruiter PC. Stability in real food webs: Weak links in long loops. Science 2002;296(5570):1120–3.
[4] Brose U, Williams RJ, Martinez ND. Allometric scaling enhances stability in complex food webs. Ecol Lett 2006;9(11):1228–36.
[5] Kartascheff B, Heckmann L, Drossel B, Guill C. Why allometric scaling enhances stability in food web models. Theor Ecol 2010;3(3):195–208.
[6] Yodzis P. The stability of real ecosystems. Nature 1981;289(5799):674–6.
[7] Heckmann L, Drossel B, Brose U, Guill C. Interactive effects of body-size structure and adaptive foraging on food-web stability. Ecol Lett 2012;15(3):243–50.
[8] Leibold MA, Holyoak M, Mouquet N, Amarasekare P, Chase J, Hoopes M, et al. The metacommunity concept: A framework for multi-scale community ecology. Ecol Lett 2004;7(7):601–13.
[9] Briggs CJ, Hoopes MF. Stabilizing effects in spatial parasitoid–host and predator–prey models: A review. Theor Popul Biol 2004;65(3):299–315.
[10] Gravel D, Massol F, Leibold MA. Stability and complexity in model meta-ecosystems. Nature Commun 2016;7(1):1–8.
[11] Brown JH, Kodric-Brown A. Turnover rates in insular biogeography: Effect of immigration on extinction. Ecology 1977;58(2):445–9.
[12] Fox JW, Vasseur D, Cotroneo M, Guan L, Simon F. Population extinctions can increase metapopulation persistence. Nat Ecol Evol 2017;1(9):1271–8.
[13] Maser GL, Guichard F, McCann KS. Weak trophic interactions and the balance of enriched metacommunities. J Theoret Biol 2007;247(2):337–45.
[14] Buckling A, Kassen R, Bell G, Rainey PB. Disturbance and diversity in experimental microcosms. Nature 2000;408(6815):961–4.
[15] Chesson P, Huntly N. The roles of harsh and fluctuating conditions in the dynamics of ecological communities. Amer Nat 1997;150(5):519–53.
[16] Mougi A, Kondoh M. Food-web complexity, meta-community complexity and community stability. Sci Rep 2016;6.
[17] Gouhier TC, Guichard F, Gonzalez A. Synchrony and stability of food webs in metacommunities. Amer Nat 2010;175(2):E16–34.
[18] Steiner CF, Stockwell RD, Kalaimani V, Aqel Z. Dispersal promotes compensatory dynamics and stability in forced metacommunities. Amer Nat 2011;178(2):159–70.
[19] Abbott KC. A dispersal-induced paradox: Synchrony and stability in stochastic metapopulations. Ecol Lett 2011;14(11):1158–69.
[20] Plitzko SJ, Drossel B. The effect of dispersal between patches on the stability of large trophic food webs. Theor Ecol 2015;8(2):233–44.
[21] Strogatz SH. Exploring complex networks. Nature 2001;410(6825):268–76.
[22] Holland MD, Hastings A. Strong effect of dispersal network structure on ecological dynamics. Nature 2008;456(7223):792–4.
[23] Hata S, Nakao H, Mikhailov AS. Dispersal-induced destabilization of metapopulations and oscillatory Turing patterns in ecological networks. Sci Rep 2014;4.
[24] Brechtel A, Gramlich P, Ritterskamp D, Drossel B, Gross T. Master stability functions reveal diffusion-driven pattern formation in networks. Phys Rev E 2018;97(3):032307.
[25] Melián CJ, Bascompte J. Food web structure and habitat loss. Ecol Lett 2002;5:37–46.
[26] Amarasekare P. Spatial dynamics of foodwebs. Annu Rev Ecol Evol Syst 2008;39:479–500.
[27] Marleau JN, Guichard F, Loreau M. Meta-ecosystem dynamics and functioning on finite spatial networks. Proc R Soc Lond [Biol] 2014;281(1777):20132094.
[28] Liao J, Bearup D, Blasius B. Food web persistence in fragmented landscapes. Proc R Soc Lond [Biol] 2017;284(1859):20170350.
[29] Yodzis P, Innes S. Body size and consumer-resource dynamics. Amer Nat 1992;1151–75.
[30] Williams RJ, Martinez ND. Simple rules yield complex food webs. Nature 2000;404(6774):180–3.
[31] Lin Y, Sutherland WJ. Color and degree of interspecific synchrony of environmental noise affect the variability of complex ecological networks. Ecol Model 2013;263:162–73.
[32] Gellner G, McCann KS. Consistent role of weak and strong interactions in high-and low-diversity trophic food webs. Nature Commun 2016;7(1):1–7.
[33] Hayes SM, Anderson KE. Beyond connectivity: How the structure of dispersal influences metacommunity dynamics. Theor Ecol 2018;11(2):151–9.
[34] Hindmarsh AC. Odepack, A Systematized Collection of ODE Solvers. IMACS Transactions on Scientific Computation, 1, Amsterdam: North-Holland; 1983, p. 55–64.
[35] Hayes SM. Metacommunity simulations in C++. Comput Code 2017. http://dx.doi.org/10.5281/zenodo.6062203.
[36] Amarasekare P, Nisbet RM. Spatial heterogeneity, source-sink dynamics, and the local coexistence of competing species. Amer Nat 2001;158(6):572–84.
[37] Levin SA. Population dynamic models in heterogeneous environments. Annu Rev Ecol Syst 1976;7(1):287–310.
[38] McCann KS, Rasmussen JB, Umbanhowar J. The dynamics of spatially coupled food webs. Ecol Lett 2005;8(5):513–23.
[39] Pillai P, Gonzalez A, Loreau M. Metacommunity theory explains the emergence of food web complexity. Proc Natl Acad Sci 2011;108(48):19293–8.
[40] Turing AM. The chemical basis of morphogenesis. Philos Trans R Soc Lond [Biol] 1952;237(641):37–72.
[41] McCullen N, Wagenknecht T. Pattern formation on networks: From localised activity to turing patterns. Sci Rep 2016;6(1):1–8.
[42] Nakao H, Mikhailov AS. Turing patterns in network-organized activator-inhibitor systems. Nat Phys 2010;6(7):544–50.
[43] Wolfrum M. The turing bifurcation in network systems: Collective patterns and single differentiated nodes. Physica D Nonlinear Phenomena 2012;241(16):1351–7.
[44] Hayes SM, Anderson KE. Predicting pattern formation in multilayer networks. Bull Math Biol 2020;82(1):1–16.
[45] Anderson KE, Hayes SM. The effects of dispersal and river spatial structure on asynchrony in consumer–resource metacommunities. Freshwat Biol 2018;63(1):100–13.
[46] dos Anjos L, Costa MIdS, Almeida RC. Characterizing the existence of hydra effect in spatial predator-prey models and the influence of functional response types and species dispersal. Ecol Model 2020;428:109109.
[47] Bajeux N, Ghosh B. Stability switching and hydra effect in a predator–prey metapopulation model. Biosystems 2020;198:104255.
[48] Mougi A. Diversity of biological rhythm and food web stability. Biol Lett 2021;17(2):20200673.
[49] Mougi A. Infected food web and ecological stability. Sci Rep 2022;12(1):1–6.
[50] Theis K, Quévreux P, Loreau M. Nutrient cycling and self-regulation determine food web stability. Funct Ecol 2022;36(1):202–13.
[51] Nonaka E, Kuparinen A. A modified niche model for generating food webs with stage-structured consumers: The stabilizing effects of life-history stages on complex food webs. Ecol Evol 2021;11(9):4101–25.
[52] Strogatz SH. From Kuramoto to crawford: Exploring the onset of synchronization in populations of coupled oscillators. Physica D Nonlinear Phenomena 2000;143(1):1–20.
[53] Gilarranz LJ, Bascompte J. Spatial network structure and metapopulation persistence. J Theoret Biol 2012;297:11–6.
[54] Gilarranz LJ, Hastings A, Bascompte J. Inferring topology from dynamics in spatial networks. Theor Ecol 2015;8(1):15–21.
[55] Gross T, Allhoff KT, Blasius B, Brose U, Drossel B, Fahimipour AK, et al. Modern models of trophic meta-communities. Philos Trans R Soc B 2020;375(1814):20190455.

[56] Hartfelder J, Reynolds C, Stanton RA, Sibiya M, Monadjem A, McCleery RA, et al. The allometry of movement predicts the connectivity of communities. Proc Natl Acad Sci 2020;117(36):22274–80.
[57] Jenkins DG, Brescacin CR, Duxbury CV, Elliott JA, Evans JA, Grablow KR, et al. Does size matter for dispersal distance? Global Ecol Biogeogr 2007;16(4):415–25.
[58] Stevens VM, Whitmee S, Le Galliard J-F, Clobert J, Böhning-Gaese K, Bonte D, et al. A comparative analysis of dispersal syndromes in terrestrial and semi-terrestrial animals. Ecol Lett 2014;17(8):1039–52.
[59] Rooney N, McCann K, Gellner G, Moore JC. Structural asymmetry and the stability of diverse food webs. Nature 2006;442(7100):265–9.
[60] Brechtel A, Gross T, Drossel B. Far-ranging generalist top predators enhance the stability of meta-foodwebs. Sci Rep 2019;9(1):1–15.
[61] Anderson KE, Fahimipour AK. Body size dependent dispersal influences stability in heterogeneous metacommunities. Sci Rep 2021;11(1):1–12.
[62] Kareiva P. Population dynamics in spatially complex environments: Theory and data. Philos Trans R Soc Lond [Biol] 1990;330(1257):175–90.
[63] Murray J. II. Spatial Models and Biomedical Applications. Springer; 2003.
[64] Rietkerk M, Van de Koppel J. Regular pattern formation in real ecosystems. Trends Ecol Evolut 2008;23(3):169–75.
[65] Pedersen EJ, Marleau JN, Granados M, Moeller HV, Guichard F. Nonhierarchical dispersal promotes stability and resilience in a tritrophic metacommunity. Amer Nat 2016;187(5):E116–28.